Structures 82 (2025) 110800

Contents lists available at ScienceDirect

Structures

journal homepage: www.elsevier.com/locate/structures

Kinematic analysis of façade collapse mechanisms in historic churches: The case of Sorrento (Naples, Italy)

Luigi Amitrano [1], Giovanna Longobardi [2], Antonio Formisano [*,3]

Department of Structures for Engineering and Architecture, University of Naples "Federico II", Piazzale Tecchio 80, Naples 80125, Italy

ARTICLE INFO

Keywords:
Cultural heritage preservation
Masonry churches
Seismic vulnerability
Kinematic analysis
Façade overturning
Slenderness factor

ABSTRACT

This study investigates the seismic vulnerability of masonry churches located in the municipality of Sorrento, a region of notable architectural heritage within the metropolitan area of Naples. The research is divided into two main phases. The first phase involved a comprehensive survey and systematic cataloguing of all religious buildings within the study area, using CarTiS forms at both the first and second levels. The first-level forms were employed to delineate territorial units and classify churches based on homogeneous architectural typologies, while the second-level forms provided detailed documentation of each building's structural characteristics. The second phase focused on assessing seismic vulnerability, with particular emphasis on the out-of-plane overturning of main facades, a frequent failure mechanism in masonry churches during earthquakes. A simplified nonlinear kinematic model was utilized, modelling the façade as an isolated masonry panel rotating around a cylindrical hinge at its base. The analysis also incorporated horizontal thrusts exerted by arches and domes on the façade. This methodological framework enables a preliminary yet meaningful evaluation of the seismic safety of the studied churches. The results reveal a strong correlation between façade geometry, slenderness, and seismic vulnerability, offering critical insights into the stability of these elements under site-specific seismic conditions. The findings support the identification of structural weaknesses and inform the development of targeted retrofitting strategies aimed at improving seismic resilience and safeguarding the region's historic architectural heritage.

1. Introduction

1.1. Seismic vulnerability of religious buildings in the Italian Peninsula

The Italian territory is characterized by an extensive presence of religious buildings, which constitute approximately 80 % of the nation's architectural heritage and plays a crucial role in shaping its historical and cultural identity [1]. According to the most recent census data, Italy is home to an estimated 95,000 churches, the vast majority of which (around 90 %) were constructed prior to the 20th century [2]. This statistic is particularly significant, as it implies that most of these structures were built without any seismic design considerations, having been conceived solely to withstand gravitational loads, and are therefore highly vulnerable to seismic events [3–5].

The construction materials commonly used in these buildings often exhibit poor mechanical properties, further compromising their seismic performance. Moreover, churches typically feature large, uninterrupted interior spaces, an absence of internal spine walls and intermediate floors, and high-slenderness walls. Many have undergone successive modifications and additions over time—factors that collectively heighten their susceptibility to earthquake-induced damage [6–14].

Given the severe damage inflicted on this irreplaceable heritage by past seismic events, it is essential to analyse the seismic behaviour of these structures and develop retrofitting strategies that enhance safety while preserving their historical and artistic value.

The first major contribution to the seismic assessment of churches was made following the 1976 Friuli earthquake [15]. The adopted methodology was structured into three key phases: a) A detailed survey of the building using a dedicated form to document geometry, materials, and crack patterns;

* Corresponding author.
E-mail address: antoform@unina.it (A. Formisano).
1 0009-0001–6384-912X
2 0000-0003–2600-8417
3 0000-0003–3592-4011

https://doi.org/10.1016/j.istruc.2025.110800
Received 7 August 2025; Received in revised form 25 November 2025; Accepted 25 November 2025
Available online 5 December 2025

b) Division of the structure into macro-elements, which are structurally independent and seismically homogeneous components such as facades, apses, bell towers, etc.;

c) Identification of potential damage modes and collapse mechanisms for each macro-element.

This approach facilitated a comprehensive understanding of earthquake-induced damage and enabled the identification of recurring vulnerabilities specific to masonry churches [1].

Subsequent seismic events, notably the 1987 Emilia-Romagna earthquake, saw the continued application of this church-specific assessment methodology. These applications revealed that churches often exhibit greater seismic vulnerability than residential buildings constructed with similar materials [16]. The accumulation of post-earthquake data eventually led to the development of a more refined methodology, systematizing the types of damage typically observed in churches and identifying eighteen characteristic collapse mechanisms [17].

This methodology was later updated and formalized as Model A–DC by the Decree of the President of the Council of Ministers (February 23, 2006), published in the Official Gazette on March 7, 2006 (No. 55). The revision expanded the damage mechanisms from eighteen to twenty-eight categories [18].

In recent years, the growing attention to the protection of architectural heritage has led to the development of numerous methods for assessing the seismic vulnerability of masonry churches and other masonry constructions, since earthquakes could cause enormous losses under both economic and social viewpoints [19]. As highlighted in the research conducted by Li et al. [20], different approaches have been developed and applied to a wide range of building types, including reinforced concrete, masonry, and timber structures, under both main shocks and aftershock sequences. Probabilistic and statistical models are widely used to estimate the dynamic response of buildings [21]. Numerical simulations and 3D modelling techniques [22] allow to simulate structural response and potential damage under seismic loads. Dynamic analyses further enable the evaluation of the vulnerability under complex loading scenarios [23]. In parallel, machine learning and data-driven approaches have gained prominence [24]. Additionally, a multi-level approach for the rapid assessment of seismic vulnerability of historic masonry structures, combining limit analysis and nonlinear dynamic analysis, has been proposed in [25]. Traditional empirical methods and visual inspections remain important, particularly for field data collection and analyses based on regional seismic standards. Historical damage data are often used to develop vulnerability models that reflect real-world performance under earthquakes. By combining probabilistic, numerical, data-driven, and empirical approaches, researchers can achieve a comprehensive understanding of seismic vulnerability and support more effective risk mitigation strategies.

In addition to these refined modelling approaches, large-scale analyses represent a valuable tool for seismic vulnerability assessment, offering an initial framework that highlights the most critical situations requiring more detailed evaluation. In this context, simplified methods rely on easily obtainable indices, which may be based on geometric parameters or derived from the EL1 procedure proposed by IGCH, such as the acceleration factor (f_a) and the seismic safety index (I_{SS}) [26–28].

Nonetheless, the seismic assessment of masonry churches remains a complex challenge in the field of structural engineering, as these buildings are often part of larger ecclesiastical complexes, including rectories, monasteries, or canon houses, along with adjacent or integrated bell towers.

1.2. Purposes and limitations of the current investigation

In response to these challenges, the present study focuses on evaluating the overturning mechanisms—frequently documented in post-earthquake surveys—that affect the main facades of churches located in Sorrento and its surrounding areas. The analysis centers on the relationship between the collapse multiplier and the slenderness factor, the latter defined as the ratio of façade height to wall thickness.

The investigation focused on a set of religious buildings located in the Sorrento area. Geometric and structural data were obtained from an extensive knowledge acquisition phase using both levels of the CarTiS forms, developed by the Italian Department of Civil Protection in collaboration with the PLINVS research centre [29]. The first-level form categorizes territorial sectors and classifies churches based on construction period, structural system, and plan configuration. The second-level form gathers detailed information for each individual building, including urban context, façade configuration, bell tower placement, and records of past interventions.

Following data collection, preliminary linear kinematic analyses were performed to determine the collapse multipliers for all surveyed facades using simplified assumptions. These results were then compared against the slenderness parameters obtained from geometric measurements. The graphical comparison clearly demonstrated the high susceptibility of these masonry facades to overturning mechanisms, revealing a critical structural condition in a significant number of the surveyed churches and underscoring the urgent need for targeted retrofitting strategies to safeguard this vulnerable and invaluable architectural heritage.

A key strength of linear kinematic analysis is its speed and simplicity, which allows initial evaluations and vulnerability estimates to be carried out quickly, even in particularly critical situations. This makes the method suitable for large-scale studies and screenings of historical heritage. However, this approach has some inherent limitations. First, the simplifying assumptions underlying the analysis, such as considering masonry with no tensile strength, infinite compressive strength, and a hinge conventionally located at the base of the façade, may lead to an overestimation of vulnerability. Moreover, the façade is treated as an isolated macro-element, neglecting its interaction with transverse walls, diaphragms, and tie rods, while dynamic effects, such as resonance or the temporal variability of seismic action, are not considered.

Despite these limitations, the simplicity of the method enabled a systematic application to a homogeneous sample of historic churches, integrating typological data from the CarTiS forms. In this context, linear kinematic analysis does not replace advanced numerical one, but serves as a territorial screening tool, useful for guiding intervention priorities and supporting more detailed studies of masonry churches which represent an invaluable cultural patrimony.

As shown in Fig. 1, churches are extensively distributed throughout the Italian Peninsula. Notably, a significant number are situated in areas of high seismic hazard along the Apennine belt, as well as in the Naples region, which is further exposed to considerable volcanic risk. The first figure was obtained by superimposing the seismic hazard map of the Italian territory with the map showing the density of churches, expressed per 10 Km^2. The second, instead, focuses on the Campania region.

In the Campania region, as depicted in Fig. 2, there is a total of 4424 religious buildings. The Province of Naples has the highest church density in the region, with approximately 0.95 churches per square kilometre, significantly exceeding the densities recorded in the provinces of Caserta (0.31), Salerno (0.29), Avellino (0.25), and Benevento (0.17). On average, the church density in Naples is nearly three times greater than that observed in the surrounding provinces.

Focusing on the Sorrentine Peninsula, as illustrated in Fig. 3, this area stretches from the Lattari Mountains to Punta Campanella and includes six municipalities: Vico Equense, Meta, Piano di Sorrento, Sant'Agnello, Sorrento, and Massa Lubrense. The church density within this region exceeds the average recorded for the Province of Naples. In total, the Sorrentine Peninsula contains approximately 137 churches, corresponding to an average density of two churches per square kilometre. The highest concentrations are found in the municipalities of Meta (4.0 churches/km^2), Sant'Agnello (3.4 churches/km^2), and Sorrento (2.7 churches/km^2).

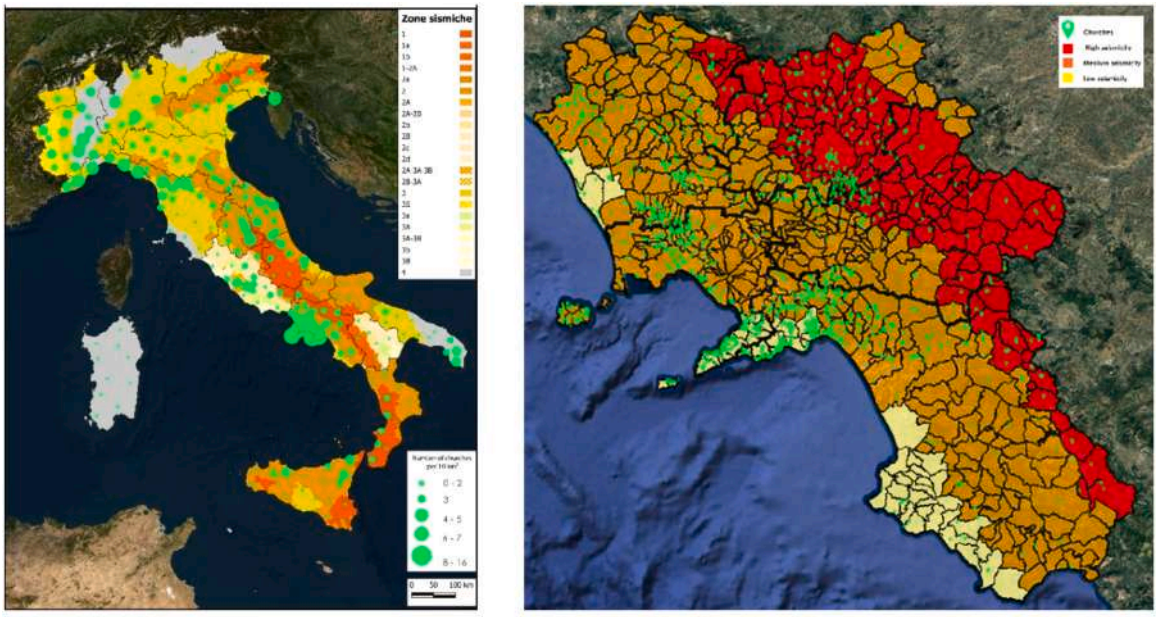

Fig. 1. a) Territorial density of churches in Italian dioceses [30] on the Seismic Hazard Map developed by Department of Civil Protection [31] and b) Placement of churches in Campania [32] with respect to the seismic classification of the region [33].

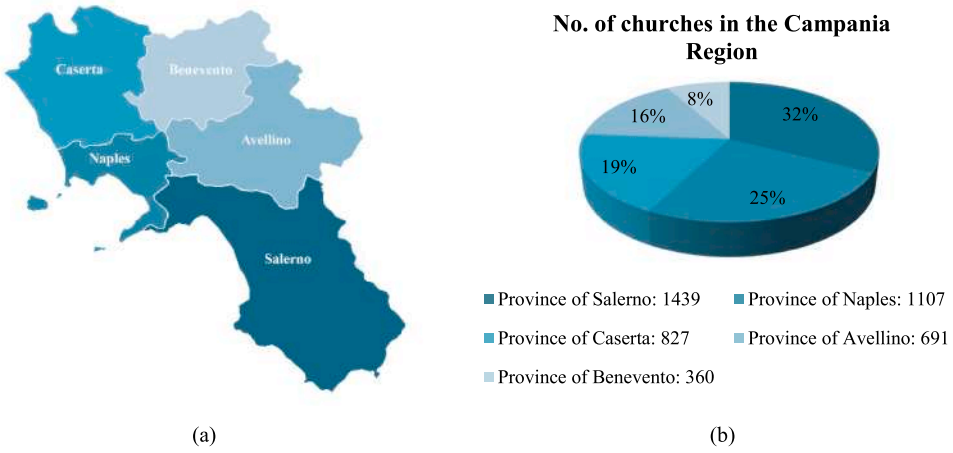

Fig. 2. a) Provinces of the Campania region, b) Number of churches in the provinces of the Campania region of Italy.

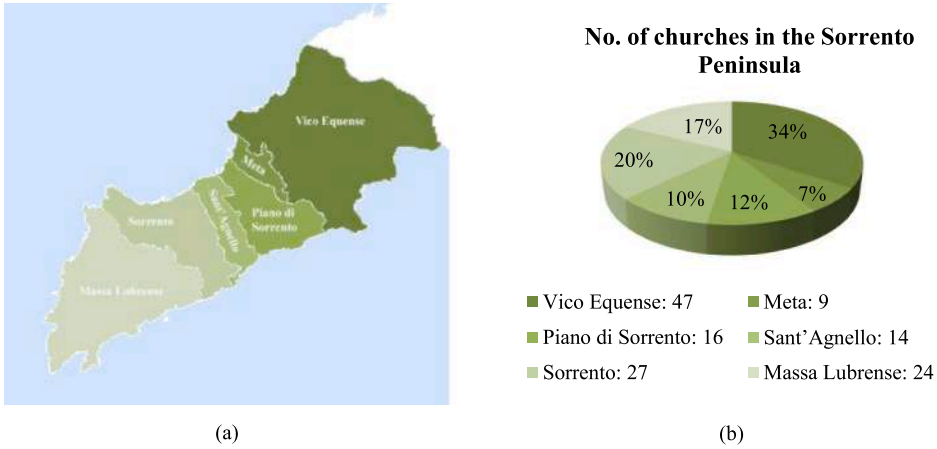

Fig. 3. a) Municipalities in the Sorrentine Peninsula; b) Number of churches in the single municipalities of the Sorrentine Peninsula.

2. The knowledge of the masonry churches through the CarTiS form

2.1. Individuation of the compartments via First Level Form

To enable a meaningful comparison between collapse multipliers and slenderness parameters, a comprehensive understanding of the buildings included in the dataset was essential. Geometric, architectural, and structural data were collected using the CarTiS forms. All ecclesiastical buildings analysed are located in the municipality of Sorrento, part of the Metropolitan City of Naples in the Campania region. Sorrento is predominantly situated on a tuffaceous terrace overlooking the Gulf of Naples. The municipality spans an area of approximately 9 km^2 and has a population of around 16,000 residents.

Fig. 4 shows the geographic location of Sorrento, along with a detailed representation of its municipal territory.

The first-level CarTiS form was used to delineate distinct territorial sectors within the municipality of Sorrento and to classify the churches according to their typological characteristics.

As illustrated in Fig. 5, three primary sectors were identified:

- Historic Centre (HC, in red): This sector encompasses the original urban core, which was historically enclosed by city walls, now partially demolished.
- Expansion Area (EA, in blue): This sector corresponds to urban developments that extended beyond the boundaries of the former city perimeter.
- Villages (V, in yellow): This area includes smaller historic centers associated with adjacent settlements.

Based on a range of parameters, including vertical structural systems, construction period, planimetric configuration, and covered surface area, the churches were classified into five distinct typologies. The distribution of churches among these categories is presented in the pie chart shown in Fig. 6 where the churches are distinguished based on their construction material, according to the following classification:

- **MUR1**: Masonry in grey tuff with squared ashlars.
- **MUR2**: Mixed masonry composed of grey tuff ashlars and stones.
- **CAR1**: Reinforced concrete structure.

The five typological categories are defined as follows:

- **T01 Category**: This group comprises large churches characterized by a Latin cross plan, three internal naves, a total area exceeding 1000 square meters, and regular grey tuff masonry. Only two churches fall into this category.
- **T02 Category**: Churches in this group feature a Latin cross plan with a central layout and side chapels, a covered area ranging from 300 to 999 square meters, and regular tuff masonry. This typology also includes two buildings.
- **T03 Category**: This typology consists of churches with a single-nave rectangular layout, a covered area between 300 and 999 square meters, and regular tuff masonry. Six churches belong to this category.
- **T04 Category**: The most common typology, comprising eleven churches, is defined by a single-nave rectangular layout, a floor area between 100 and 299 square meters, and regular tuff masonry.
- **T05 Category**: This group includes more recent churches constructed in the second half of the 20th century, typically using reinforced concrete structures. These buildings cover areas between 300 and 999 square meters. Two churches are classified under this category.

In addition to these five main categories, four churches exhibit unique architectural and structural characteristics that prevent their

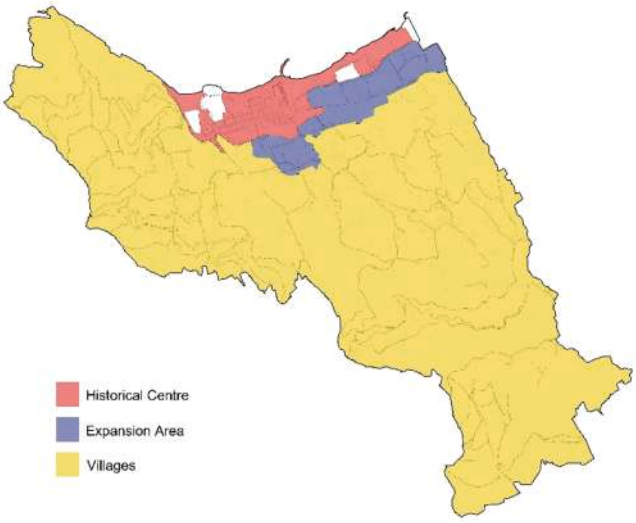

Fig. 5. Identification of sectors within the territory of Sorrento.

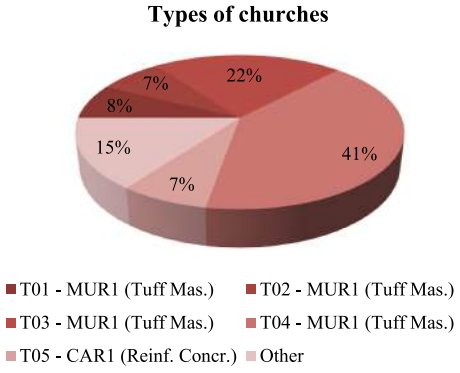

Fig. 6. Percentage distribution of the different typological categories of churches.

Fig. 4. a) Placement of the Sorrento municipality within the Campania region; b) Enlarged map of the city of Sorrento.

inclusion in the above typologies:

- *Church of the Addolorata*: characterized by a Greek cross plan.
- *Church of Santa Maria de Restilianis*: features an elliptical central plan.
- *Church of Sant'Atanasio*: includes two internal naves and vertical structures composed of tuff and stone masonry.
- *Church of Santa Maria della Purità*: also constructed with tuff and stone masonry.

The last two churches also differ notably in size compared to the categorized typologies.

Most of the data were collected through on-site inspections, interviews with the parish priests, and consultation of online sources [34] (Fig. 7).

2.2. Structural properties through the second level CarTiS form

The twenty-seven churches included in the dataset were further examined using the second level of the CarTiS form, specifically the *CarTiS Churches* sheet, which was developed to facilitate detailed data collection for religious buildings.

The second level of the form enables the collection of more detailed information on the geometric and structural characteristics of the churches. The first section records the location data and identifies the diocese to which each church belongs. In the present case, the reference Archdiocese is Sorrento–Castellammare di Stabia, which includes 88 parishes (organized into four vicariates), serves a population of approximately 245,000 inhabitants, and covers an area of 205 km^2. This section also gathers information on the church's placement within the urban context, site characteristics, and access routes.

2 documents the geometric layout, including the typology of the plan, the presence or absence of a bell tower, and, if present, its location relative to the main structure. Further details are requested regarding the number of internal naves, the presence of lateral chapels, and the shape of the apse.

The subsequent parts of the form focus on the structural properties of the church, each dedicated to a specific construction typology. 3.1 is intended for masonry churches or those with mixed structural systems, while 3.2 refers to reinforced concrete religious buildings. For the former, the form also collects information on the types of vaults and any domes present. Finally, this level of the form gathers data on openings, staircases, roof structures, and foundations, along with an assessment of the building's conservation state.

Analysis of the collected data revealed that in 89 % of cases, the original construction dates back to before the 19th century, with a concentration in the 16th and 17th centuries, as illustrated in the pie chart in Fig. 5a.

Structurally, 85 % of the churches feature vertical elements composed of grey tuff masonry laid in a regular arrangement (Fig. 5b), with wall thicknesses varying between 50 and 100 cm. Only two churches present a hybrid structural system, combining masonry with a reinforced concrete frame.

From an architectural standpoint, the most prevalent plan layout is rectangular, observed in 59 % of the buildings (Fig. 5c), followed by the Latin cross plan. Additionally, a single nave is the dominant spatial configuration, found in 82 % of the sample (Fig. 5d), while only 7 % of the churches have more than two internal naves.

As for the main façade, the most frequently observed typology is the double-pitched façade, present in 33 % of the sample (Fig. 5e). The second most common type, accounting for 29 %, includes facades featuring semi-columns or other architectural elements attached to the external surface. Other façade configurations appear in smaller proportions.

Table 1 lists the masonry churches included in the study along with their denominations, classified according to their location within the defined homogeneous compartments. In this context, HC denotes the Historic Centre, EA refers to the Expansion Area, and V indicates Villages.

3. Methodology of the work

3.1. Calculation criteria for assessing overturning phenomena of main facades

Following a seismic event, the extent of damage sustained by a masonry church can vary widely depending on structural configuration, construction quality, and seismic intensity.

In the minor damage state, cracks typically form in the upper portions of the nave walls, particularly near the connection with the façade or around corner openings. These cracks do not extend to the base of the wall and may be visible on both interior and exterior surfaces.

In the moderate damage state, through-cracks propagate down to the wall base, indicating partial detachment between the façade and the longitudinal walls. This behaviour is usually localized at the corners or near adjacent openings, suggesting compromised connectivity between structural elements.

The severe damage state is characterized by a similar crack distribution but accompanied by significant out-of-plumb displacement of the façade and wider through-cracks, indicating an advanced stage of structural deformation and instability [1].

The overturning of main facades is among the most common out-of-plane failure mechanisms observed in masonry churches. This vulnerability is primarily due to the absence of longitudinal tie rods, poor connection between the top of the façade and the roof structure (e.g., lack of ring beams or bracing systems), and inadequate anchorage between the façade and adjoining walls, that are all indicative of the absence of the so-called *box-like behaviour* [6]. Furthermore, churches were often constructed in multiple phases, with the façade almost being the final element to be completed. This allowed for aesthetic updates, reflecting contemporary architectural styles, and adjustments based on available resources.

Generally, façade collapse occurs as a result of the loss of equilibrium of the masonry panel, leading to the formation of a cylindrical hinge at the wall base, as illustrated by the example shown in Fig. 8.

To evaluate the susceptibility of the main facades of the masonry churches in the dataset to overturning phenomena, and to examine the relationship with the slenderness parameter, a linear kinematic approach was employed. In this method, each façade is idealized as a rigid block rotating about a hinge located at its base. In this preliminary phase, this assumption is reasonably realistic, since most buildings did not show the presence of rigid diaphragms, horizontal ties, or thrusting vaults, suggesting that rotation is more likely to occur at the base.

However, recent studies have highlighted that the hinge position governing overturning varies with façade geometry, boundary conditions, openings, and diaphragm stiffness [25].

The analysis follows the classical assumptions of limit analysis, namely: zero tensile strength, infinite compressive strength, and no sliding between masonry units [34,35].

These simplifying hypotheses influence the estimation of vulnerability. Considering masonry with no tensile strength leads to immediate crack opening, overestimating out-of-plane fragility. Assuming infinite compressive strength excludes local crushing, attributing collapse only to overturning or sliding, which may underestimate some real mechanisms. The absence of friction between blocks allows free sliding, further increasing the overestimation of vulnerability. In summary, these simplifications make the model conservative and suitable for preliminary assessments, but the results should not be interpreted as absolute safety estimates [36,37].

Within this framework, each overturning mechanism is modelled as a kinematic chain, wherein collapse is triggered by a loss of equilibrium associated with the formation of a cylindrical hinge at the base of the masonry panel.

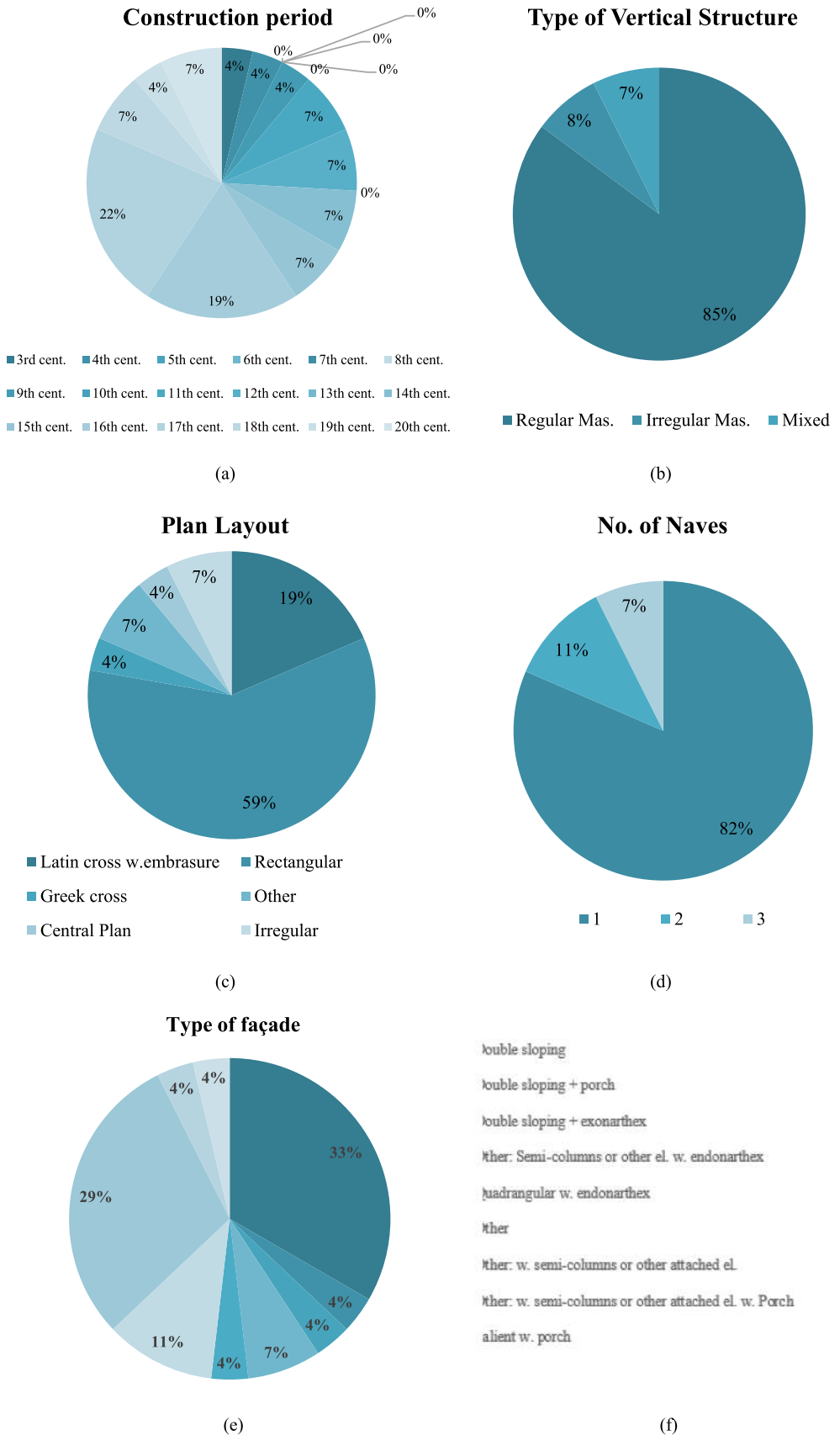

Fig. 7. Data acquired from second-level CarTiS form: a) Construction period, b) Type of vertical structure; c) Plan Layout; d) Number of naves; e) Type of façade; f) Legend.

Table 1
List of the 27 churches under investigation.

ID	Name of the church	ID	Name of the church
HC1	Cathedral of Saints Philip and James	EA1	Church of Our Lady of Lourdes
HC2	Church of St Paul	EA2	Church of St Onofrio
HC3	Church of the Annunziata	EA3	Church of St Lucia
HC4	Church of St Francesco	EA4	Church of St Pietro in Mele
HC5	Church of Saints Felice and Bacolo	EA5	Church of St Antonio
HC6	Basilica of St Antonino	V1	Church of St Maria di Montevergine
HC7	Church of Madonna delle Grazie	V2	Church of St Maria di Casarlano
HC8	Church of Addolorata	V3	Church of St Biagio
HC9	Sanctuary of the Madonna del Carmine	V4	Church of St Atanasio
HC10	Church of St Anna	V5	Church of St Maria del Toro
HC11	Church of Madonna del Soccorso	V6	Church of Madonna del Rosario
HC12	Church of S. Maria de Restilianis	V7	Church of Madonna di Constantinople
HC13	Church of St Maria della Pietà	V8	Church of St Maria della Purità
HC14	Church of Maria SS. Assunta		

Fig. 8. Example of façade overturning characterized by the formation of a cylindrical hinge at the base of the masonry wall. The case shown refers to the Church of the Addolorata, one of the buildings included in the dataset.

The choice to consider and investigate the overturning mechanism of the main façade is strongly supported by similar cases observed in churches during past seismic events that have struck Central Italy and Emilia-Romagna region [38–41]. Significant examples are illustrated by the photographic documentation provided in Fig. 9, where clear cracks were observed between the main façade and the lateral nave walls.

3.2. Evaluation of façade panels and the influence of arches and vaults

The first step of this investigation involved the acquisition of the geometric data for each façade. Specifically, the length, height and thickness, expressed in meters, were measured and recorded. Once these dimensions were known, and considering the specific weight of the construction material—tuff masonry—the volume of each masonry panel was calculated.

For the weight calculation, a unit weight equal to 16 kN/m³ was adopted, in accordance with the values provided by the Italian Technical Code [42,43].

The second phase consisted of the identification of the thrusts generated by the arches orthogonal to the plane of the façade. These horizontal forced were determined using the freely available software ARCO, which enables the calculation of arch-induces forces [44,45]. Fig. 9 provides a view from the software.

Following the determination of horizontal and vertical forces acting on the façade, the overturning and stabilizing moments were calculated using Eqs. (1) and (2), respectively. These values were then used to compute the collapse multiplier α via Eq. (3).

The collapse multiplier α is a dimensionless coefficient that quantifies the structure's capacity to resist horizontal actions before failure. A higher α\alphaα indicates a greater resistance to lateral loads, while a lower value suggests increased vulnerability and a higher likelihood of collapse under relatively small horizontal forces.

$$M_{R=\alpha[\sum_{i=1}^{n} W_i \bullet y_{Gi} + \sum_{i=1}^{n} F_{Vi\bullet} \quad h_{Vi+} \quad \sum_{i=1}^{n} P_{Si\bullet} h_i] + \sum_{i=1}^{n} F_{Hi} \bullet h_{Vi} + P_H \bullet h_i} \tag{1}$$

$$M_{S=\sum_{i=1}^{n} W_i \bullet \frac{s_i}{2} + \sum_{i=1}^{n} F_{Vi\bullet} \quad d_{Vi+} \quad \sum_{i=1}^{n} P_{Si\bullet} d_i + \sum_{i=1}^{n} T_i \bullet h_i} \tag{2}$$

$$\alpha = \frac{\sum_{i=1}^{n} W_i \bullet \frac{s_i}{2} + \sum_{i=1}^{n} F_{Vi\bullet} \quad d_{Vi+} \quad \sum_{i=1}^{n} P_{Si\bullet} d_i + \sum_{i=1}^{n} T_i \bullet h_{i-} \sum_{i=1}^{n} F_{Hi} \bullet h_{Vi} - P_H \bullet h_i}{\sum_{i=1}^{n} W_i \bullet y_{Gi} + \sum_{i=1}^{n} F_{Vi\bullet} \quad h_{Vi+} \quad \sum_{i=1}^{n} P_{Si\bullet} h_i} \tag{3}$$

where:

- W_i denotes the self-weight of the wall at the *i*-th level, or of the *i*-th microelement;
- F_{Vi} represents the vertical component of the thrust exerted by arches or vaults on the wall at the *i*-th level;
- F_{Hi} denotes the horizontal component of the thrust exerted by arches or vaults on the wall at the *i*-th level;
- P_{Si} is the weight of the floor acting on the wall at the *i*-th level;
- P_H represents the static thrust transmitted by the roof to the top of the microelement;
- T_i is the force exerted by any tie rods present at the top of the wall at the *i*-th level;
- s_i indicates the thickness of the wall at the *i*-th level;
- h_i is the vertical lever arm of the action transmitted by the floor and/or tie rod to the wall at the *i*-th level, or alternatively, the height of the *i*-th microelement;
- y_{Gi} represents the vertical lever arm of the self-weight of the *i*-th body;
- d_i is the horizontal lever arm of the load transmitted by the floor to the wall at the *i*-th level;
- h_{Vi} denotes the vertical lever arm of the thrust from arches or vaults at the *i*-th level;
- d_{Vi} is the horizontal lever arm of the actions transmitted by arches or vaults at the *i*-th level.

Fig. 10 depicts the schematic layout of the overturning mechanism, including all loads acting on the masonry panel.

In the context of kinematic analysis of rigid-body overturning collapse mechanisms, a linear displacement profile is assumed along the height of the mechanism. To implement this assumption, a unit virtual displacement is applied at the top of the structure, representing the point of maximum movement. The corresponding virtual displacements at various levels, where horizontal forces are applied, are then derived based on geometric proportionality with respect to the total height of the mechanism.

$$\delta_i : H_{tot} = \delta_{virt} : h_i \tag{4}$$

In particular, the displacement is computed using Eq.5:

$$\delta i = \frac{hi \cdot \delta_{vir}}{Htot} \tag{5}$$

where:

h_i denotes the elevation of the i-th load application point, measured vertically up to the base hinge;

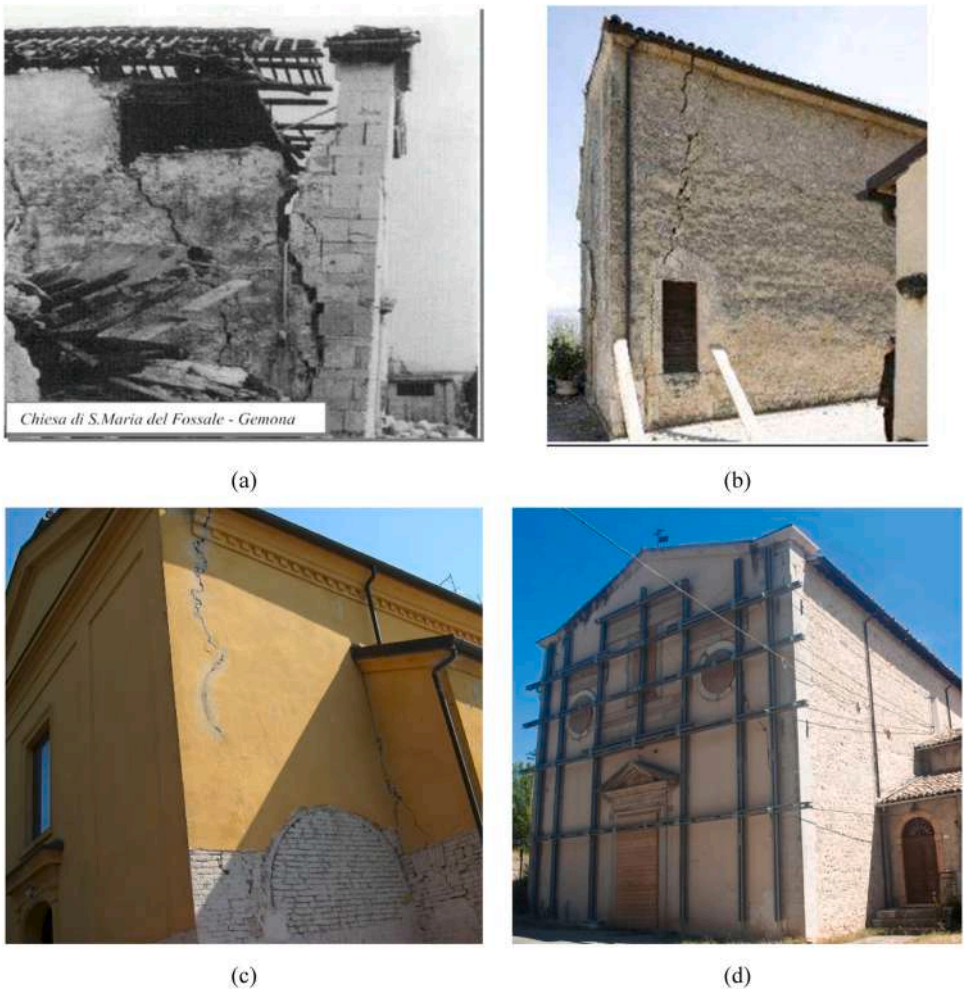

Fig. 9. a) Church of Saint Mary del Fossale (Gemona); b) Church of Santa Maria ad Criptas in Fossa (L'Aquila); c) Church of Saint Biagio in Carpi (Modena); d) Church of Saint Vito in Norcia (Perugia).

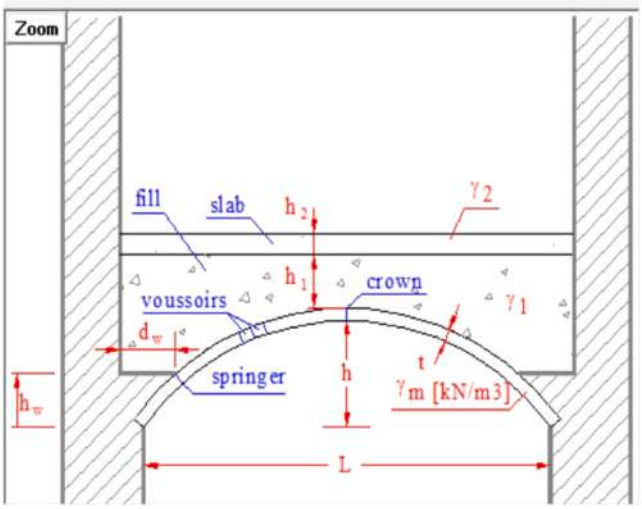

Fig. 10. Cross-section of a masonry arch and identification of the data to be inserted in the ARCO program.

H_{tot} denotes the total height of the panel, measured from the base to the topmost point.

δ_{vir} is the virtual displacement applied on the top of the masonry walls, assumed equal to 1.

After determining the horizontal forces and their respective lever arms, as well as calculating the self-weight of the masonry panel and the height of its center of gravity, the participating mass M* involved in the kinematic mechanism was computed using Eq. (6) to evaluate the panel's overturning and the corresponding capacity acceleration. From M*, the mass participation factor e* (Eq. 7) and the spectral acceleration a_0^* (Eq. 8) were subsequently derived.

The participating mass M* represents the portion of the total mass actively contributing to the collapse mechanism. It is calculated by considering only the vertical loads that correspond to the virtual displacement distribution defined by the assumed kinematic mechanism.

$$M^* = \frac{\left[\sum_i P_i \bullet \delta_{vir}\right]^2}{g \bullet \sum_i (P_i \bullet \delta_{vir}^2)} \tag{6}$$

where:

P_i represents the vertical loads acting on the structure. Under seismic conditions, these masses generate horizontal inertial forces that act on the elements of the kinematic mechanism;

δ_{vir} denotes the virtual horizontal displacement at the point of application of the i-th load P_i;

g is the acceleration due to gravity.

The participating mass factor e* represents the fraction of the element's total mass that actively contributes to the collapse mechanism. This factor is a fundamental parameter for estimating the energy

involved in the mechanism and calculating the equivalent seismic strength and it is defined as follows:

$$e^* = \frac{g \bullet M^*}{\sum_i P_i} \tag{7}$$

where:

- g is the gravity acceleration;
- M* represents the participating mass.
- P_i are the applied weight forces whose masses, as a result of the seismic actions, generate horizontal forces on the elements of the kinematic chain.

The overturning verification for each masonry panel was performed by comparing the spectral acceleration (a_0^*) with the minimum expected ground acceleration ($a_{0,min}$) by means of Eq. (8).

The check is satisfied and, thus, the masonry wall does not overturn if:

$$a_0^* \geq a_{0,min} \tag{8}$$

Spectral acceleration a_0^* is derived as follows:

$$a_0^* = \frac{\alpha_0 \cdot g}{e^* \cdot F_C} \bullet q \tag{9}$$

where:

- α_0 is the multiplier of the seismic action leading to collapse, determined using the principle of virtual works (see Eq. 3);
- g is the gravity acceleration;
- e^* is the participating mass fraction (see Eq. 7);
- F_c is the confidence factor, equal to 1.35, corresponding to knowledge level 1;
- q is the behaviour factor, assumed equal to 1 for linear analysis.

The minimum expected ground acceleration is determined by means of the following relationship:

$$a_{0,min} = \frac{a_g \bullet S}{q} \tag{10}$$

where:

- a_g is the peak ground acceleration for the city of Sorrento;
- S is the coefficient accounting for the foundation soil. In this case, a type C soil was assumed and, therefore, this coefficient takes a value of 1.50.

3.3. Geometric and structural data of the investigated churches in Sorrento

The dataset herein considered for investigation includes twenty-seven masonry churches. However, two constructions, namely Church EA1 and Church V6, were excluded from the linear analysis because of their reinforced concrete structures, as the study focused exclusively on masonry churches.

Moreover, two additional religious buildings were excluded because their facades are not independent, preventing the application of the kinematic overturning model. These are the Church of Madonna delle Grazie (HC7) and the Church of SS. Assunta (HC14), as illustrated in Fig. 11. In the case of Church HC7, access to the main nave is through a tall portico covered by a barrel vault. Above this portico is a volume containing a women's gallery, which allows members of the religious community to observe the interior while remaining separated from the outside environment (Fig. 11a).

Conversely, the main entrance of Church HC14 is located on Sersale Street and accessed via an elevated passage that runs through a portion of the building situated behind the apse of the Cathedral of Sorrento (HC1) (Fig. 11b).

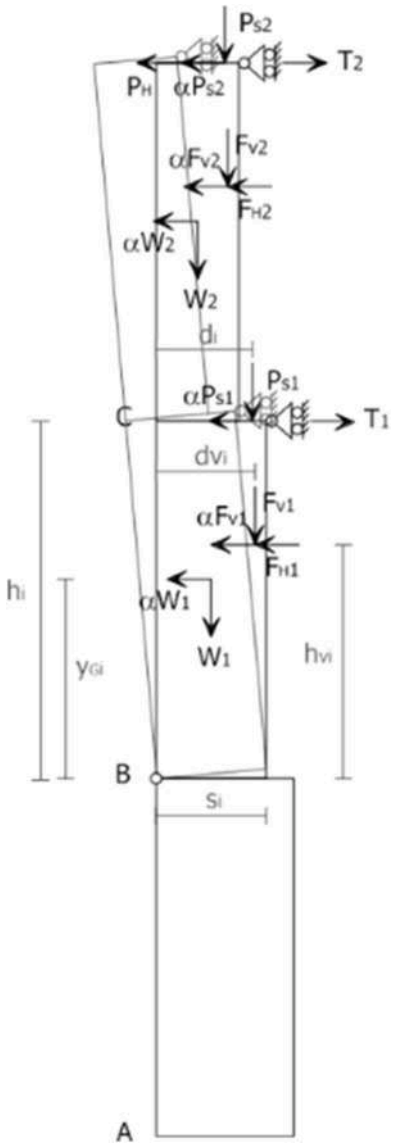

Fig. 11. Schematic representation of the main façade mechanism.

Table 2 presents each main façade through a schematic three-dimensional model created in AutoCAD 3D, accompanied by a corresponding photograph and its typology classified according to the CarTiS categories. The table further notes the presence of a bell tower, which was included in the geometrical data only when integrated in continuous alignment with the main façade, and excluded when set back or structurally detached.

Table 3 lists the geometric data for each main façade, along with the calculation of the slenderness parameter, which serves as the primary criterion for comparison. Specifically, the calculation of the volume of the façade has been conducted on the three-dimensional model created in the AutoCAD environment.

4. Evaluation of the overturning phenomena of the main facades

4.1. Safety checks

Following the initial evaluation of slenderness, the horizontal thrusts generated by the arches orthogonal to the main façade were calculated using the ARCO software. The analysis considered only those arches or

Table 2
Three-dimensional view, photographic documentation and typology of each façade.

3D View	Photo Documentation	ID	Type of façade	Bell tower
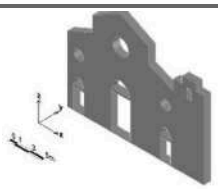		HC1	Salient with porch	Present
		HC2	Other – with semi-columns or other attached elements	Excluded
		HC3	Other – with semi-columns or other attached elements with endonarthex	Present
		HC4	Other – with semi-columns or other attached elements with endonarthex	Excluded
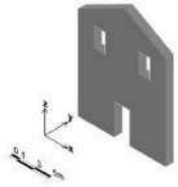		HC5	Double sloping	Excluded
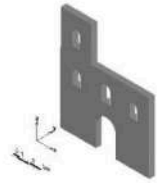		HC6	Quadrangular with endonarthex	Present
		HC8	Double sloping	Excluded
		HC9	Other – with semi-columns or other attached elements with endonarthex	Excluded

(*continued on next page*)

Table 2 (*continued*)

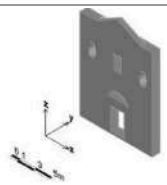		HC10	Other – with semi-columns or other attached elements	Excluded
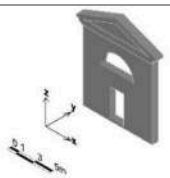		HC11	Double sloping	Excluded
		HC12	Other – with semi-columns or other attached elements	Excluded
		HC13	Other – with semi-columns or other attached elements	Excluded
		EA2	Other – with semi-columns or other attached elements	Excluded
	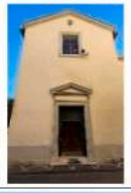	EA3	Double sloping	Excluded
		EA4	Double sloping with porch	Excluded
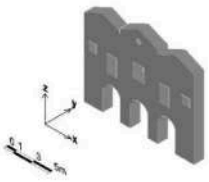	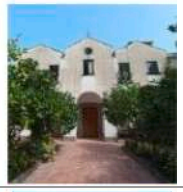	EA5	Double sloping with exonarthex	Excluded
		V1	Double sloping	Excluded

(*continued on next page*)

Table 2 (*continued*)

		V2	Double sloping	Excluded (Adjacent Structure)
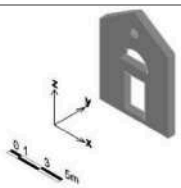		V3	Double sloping	Excluded
		V4	Other – with semi-columns or other attached elements with porch	Excluded
		V5	Double sloping	Excluded
		V7	Other	Excluded (Adjacent Structure)
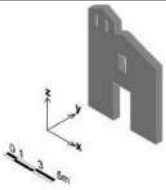		V8	Double sloping	Present

dome segments exerting direct loads on the façade. To aid interpretation, certain simplifications were introduced in both the graphical representation of the acting forces and the floor layouts of some churches, based on the available documentation.

Once the horizontal thrusts of the arches (H_i) and their corresponding lever arms (D_{pi}) were determined, alongside the weight of the wall panel (W) along with the height of its centre of gravity (Z_g) were calculated, the overturning and stabilizing moments acting on the panel were derived. These moments were then used to compute the collapse multiplier (α) in accordance with Eq. 3.

Subsequently, applying the principle of virtual work, the participating mass (M*) involved in the collapse mechanism was computed using Eq. 6, and the corresponding mass participation factor (e*) was derived from Eq. 7.

Given the level of available information, a confidence factor $F_C = 1.35$ was adopted, consistent with a limited Knowledge Level (KL1), as defined in the Italian Technical Code 2018 and its related applicative Circular.

The collapse spectral acceleration for the façade (a_0^*) was then computed using Eq. 8 and compared with the minimum required spectral acceleration ($a_{0,min}$), corresponding to the seismic input for the Sorrento site on soil type C. The overturning safety check was performed by comparing these two values. The results of this assessment are provided in Table 4 for all the investigated churches.

As shown in the table, all the church facades exhibit spectral accelerations significantly lower than the seismic demand for the site. This clearly indicates a widespread vulnerability to out-of-plane seismic actions.

The findings confirm that, without adequate structural connections between adjacent walls and proper maintenance over time, all facades are susceptible to overturning under seismic loads. These results highlight the urgent need for targeted retrofitting measures to enhance the overall stability of masonry panels in religious buildings.

It should be noted that the results attained represent only an initial, large-scale evaluation of the seismic vulnerability of the investigated churches in the municipality of Sorrento. The unsatisfactory agreement

Table 3
Geometric data of examined facades.

ID	Width	Height	Thickness	Volume	Slenderness λ
[-]	[m]	[m]	[m]	[m^3]	[-]
HC1	20.31	15.82	1.54	229.07	10.30
HC2	13.97	17.00	2.71	278.57	6.27
HC3	11.93	10.86	0.84	79.22	13.00
HC4	17.27	22.02	1.30	367.59	16.94
HC5	11.26	15.00	1.00	136.49	15.00
HC6	16.60	19.43	1.00	218.18	19.43
HC8	14.16	18.78	0.95	222.70	19.76
HC9	9.68	15.06	0.79	68.17	19.06
HC10	9.21	12.94	1.02	99.14	12.69
HC11	9.42	11.12	0.90	53.33	12.36
HC12	9.55	11.65	1.61	116.52	7.23
HC13	8.46	9.54	1.00	62.10	9.54
EA2	9.34	12.42	1.00	76.70	12.42
EA3	7.36	11.98	0.80	58.35	14.97
EA4	7.93	11.03	0.90	54.00	12.25
EA5	12.34	10.10	1.10	98.45	9.18
V1	9.24	14.03	0.60	63.78	23.39
V2	9.81	14.29	1.00	116.85	14.29
V3	6.67	9.01	0.65	28.09	13.86
V4	10.89	11.17	0.80	62.54	13.96
V5	6.12	8.26	0.80	27.58	10.33
V7	5.83	9.55	0.66	24.62	14.46
V8	7.17	9.75	0.66	34.52	14.78

Table 4
Results of the overturning phenomena checks.

ID	a_0^*	$a_{0,min}$	α	Check
[-]	[m/s^2]	[m/s^2]	[-]	[-]
HC1	0.47	1.70	0.065	Unsatisfied
HC2	0.92	1.70	0.127	Unsatisfied
HC3	0.50	1.70	0.068	Unsatisfied
HC4	0.47	1.70	0.065	Unsatisfied
HC5	0.53	1.70	0.073	Unsatisfied
HC6	0.43	1.70	0.060	Unsatisfied
HC8	0.39	1.70	0.054	Unsatisfied
HC9	0.07	1.70	0.010	Unsatisfied
HC10	0.62	1.70	0.085	Unsatisfied
HC11	0.59	1.70	0.082	Unsatisfied
HC12	1.04	1.70	0.144	Unsatisfied
HC13	0.81	1.70	0.112	Unsatisfied
EA2	0.64	1.70	0.088	Unsatisfied
EA3	0.51	1.70	0.070	Unsatisfied
EA4	0.56	1.70	0.078	Unsatisfied
EA5	0.01	1.70	0.001	Unsatisfied
V1	0.31	1.70	0.043	Unsatisfied
V2	0.41	1.70	0.056	Unsatisfied
V3	0.56	1.70	0.078	Unsatisfied
V4	0.55	1.70	0.076	Unsatisfied
V5	0.77	1.70	0.106	Unsatisfied
V7	0.56	1.70	0.077	Unsatisfied
V8	0.54	1.70	0.074	Unsatisfied

between capacity and demand accelerations demonstrated a high susceptibility to out-of-plane phenomena, primarily due to the lack of proper and adequate connections among vertical walls.

This preliminary assessment will be followed by a more comprehensive and refined seismic analysis, potentially supported by numerical modelling.

4.2. Critical analysis of the results

Fig. 12 illustrates the relationship between the two parameters, with the slenderness ratio λ plotted along the horizontal axis and the collapse multiplier α along the vertical axis. The facades are represented by coloured points, with different colours corresponding to diverse façade typologies.

The relationship between the two parameters is presented through a linear regression, which provides a simple and easily interpretable representation of the correlation between slenderness and collapse multiplier. In a preliminary large-scale assessment, this approach allows for the immediate identification of cases that deviate from the general trend.

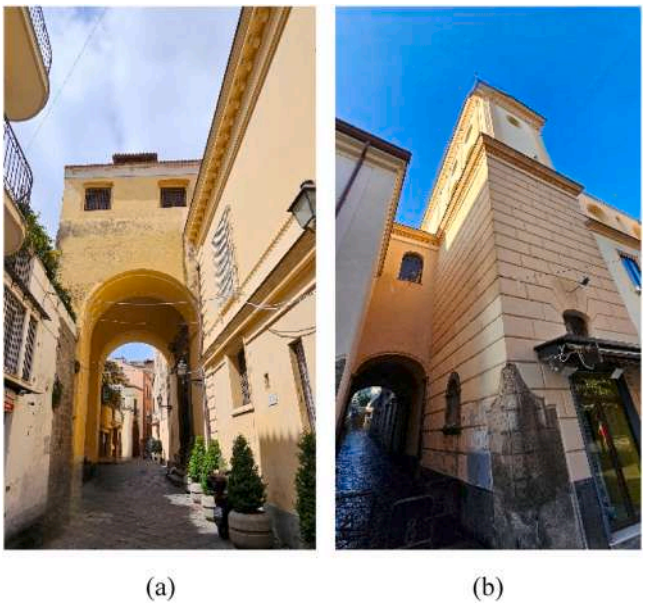

Fig. 12. Main entrance of a) Church of the Madonna delle Grazie (HC7); b) Church of Maria SS. Assunta (HC14).

The analysis reveals a clear inverse correlation between slenderness and structural capacity: as slenderness increases, the out-of-plane resistance of the façade tends to decrease. This behaviour aligns with mechanical expectations, as slender facades typically exhibit lower stability and are therefore more susceptible to out-of-plane failure mechanisms, even under relatively moderate seismic loads.

The observed trend is consistent with current regulatory guidelines, which emphasize the influence of geometric proportions, such as slenderness, on seismic vulnerability. Most of the analysed facades cluster closely around the regression line, confirming the strength of this correlation.

However, some data points deviate from the general tendency. For example, typologies V5 and HC13 show relatively low slenderness values but correspondingly high collapse multipliers, while Church HC9 also exhibits a significant deviation from the main trend. These divergences may result from factors such as substantial horizontal thrusts from internal vaulted or domed structures, advanced material degradation or damage, unfavorable local geometric irregularities, and insufficient connections between the façade and adjacent transverse structural elements.

In the following pictures the kinematic analysis results for the two most common façade typologies, namely the double-sloping type (Fig. 13) and the type featuring architectural decorative elements (Fig. 14), such as semi-columns, are presented (Fig. 15).

Even within these two subsets, an inverse correlation between slenderness and structural capacity can be observed.

Regarding the first and most common façade typology, which accounts for 33 % of the set, churches with greater slenderness tend to exhibit lower α values, indicating higher vulnerability. The dashed regression line highlights a general decreasing trend, although some local deviations are present. Interestingly, despite often being associated with simpler architectural layouts, the double-sloping façade typology does not necessarily confer better stability. The absence of restraining elements, such as ring beams or tie rods, significantly affects the out-of-plane behaviour of these facades.

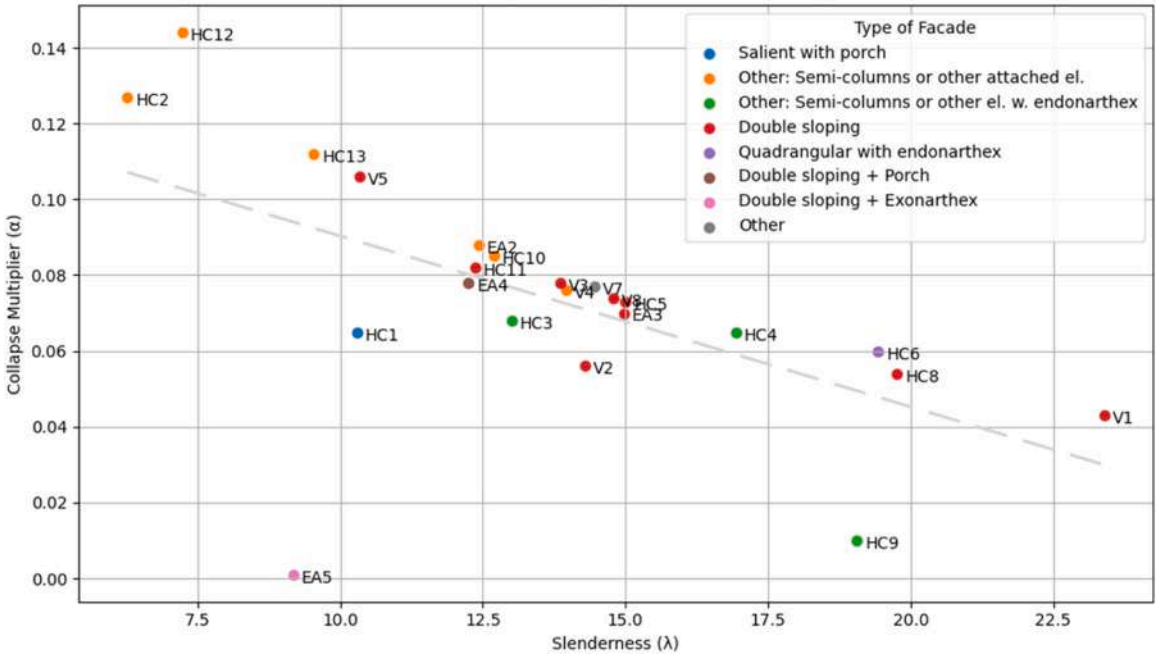

Fig. 13. Comparison between slenderness and collapse multiplier for all the typologies of facades.

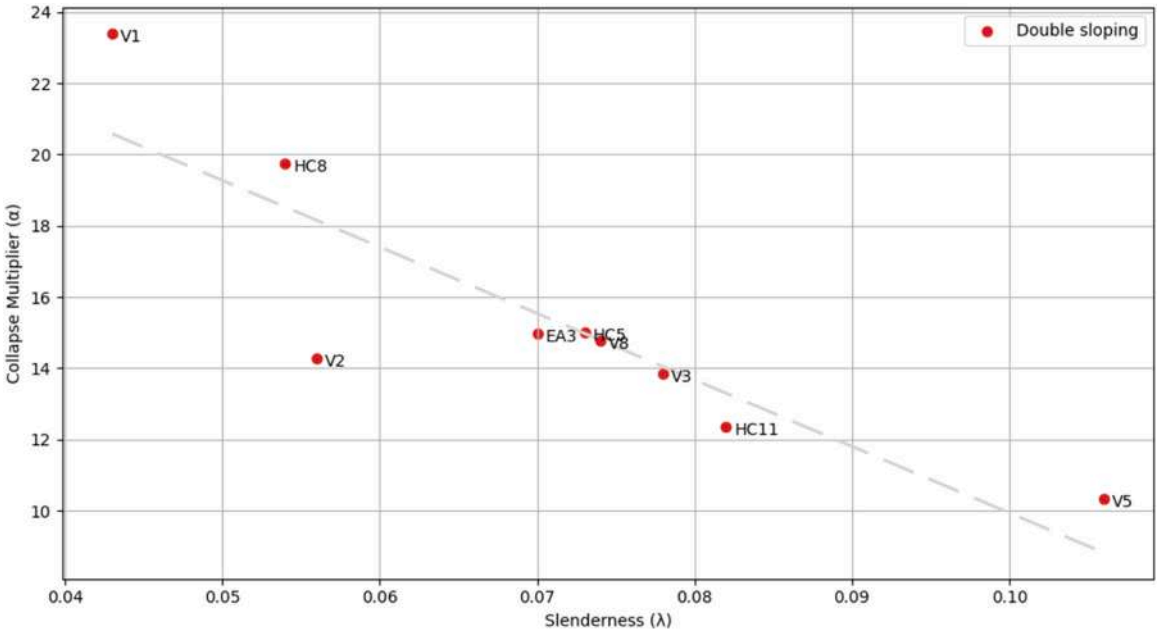

Fig. 14. Comparison between slenderness and collapse multiplier for the most frequent typology of facade (Double Sloping Façade).

The second prevalent façade typology demonstrates inconsistent performance under loading. Architectural features such as semi-columns and decorative elements, though visually prominent, offer no structural contribution unless effectively bonded to the façade. More often, they act as independent bodies, rendering them highly susceptible to transverse actions.

Moreover, the diversity of architectural configurations, ranging from porches to exonarthexes, suggests that certain features may positively influence mechanical performance, even in cases of high slenderness. This observation opens promising avenues for further research into how spatial and geometric organization affects the overall stability of historic masonry facades.

Overall, given that all facades show susceptibility to overturning and that slenderness plays a significant role in this vulnerability, further exacerbated by inadequate connections with adjacent lateral walls and the lack of box behaviour, this evaluation underscores the urgent need for targeted structural consolidation. Such interventions should be specifically designed to enhance façade stability and mitigate damage risks during seismic events.

5. Conclusions

This study investigated the relationship between geometric slenderness and the collapse multiplier of the main facades of a group of historic churches located in the municipality of Sorrento, within the metropolitan area of Naples.

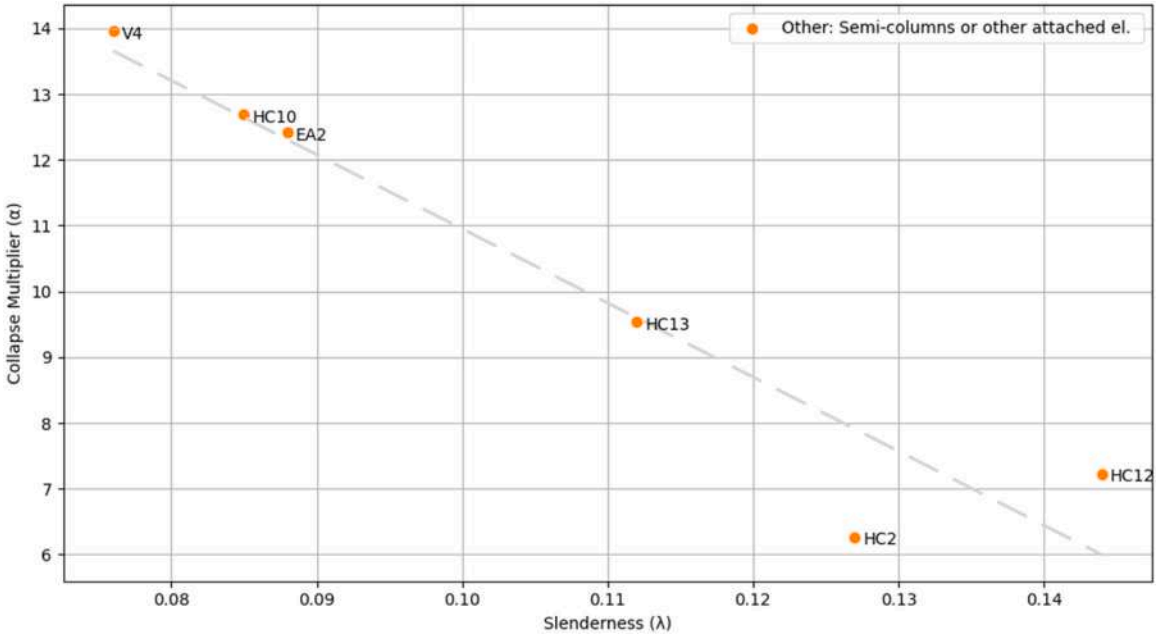

Fig. 15. Comparison between slenderness and collapse multiplier for the second most frequent typology of façade (Other typologies with semi-columns and other attached elements).

Before the analytical phase, a comprehensive knowledge acquisition process was conducted using an integrated approach based on the two levels of the CarTiS forms, enabling data collection from the territorial scale down to individual buildings. The second-level analysis revealed that the most common façade typology is the double-sloping type, present in approximately 33 % of the sample, a significant finding that reflects the prevailing morphology of the local ecclesiastical heritage.

The analysis employed a simplified linear kinematic approach, assuming masonry to have zero tensile strength and infinite compressive strength, neglecting sliding between masonry blocks. The façade was modelled as a rigid body rotating about a cylindrical hinge located at the base of the masonry panel.

Results reveal a clear inverse relationship between slenderness and the collapse multiplier: more slender facades tend to exhibit lower structural capacity. All facades analysed showed spectral acceleration values below the seismic demand for the site, with none meeting safety criteria against out-of-plane overturning. This widespread vulnerability is further aggravated by frequent absence of effective connections with adjacent transverse structures, lack of ring beams or tie rods, and significant horizontal thrusts from vaults, arches, or domes.

Some deviations from the general trend were observed, indicating unusually low or high collapse multipliers relative to the expected slenderness. These anomalies may be attributed to unfavourable local geometries, material degradation, eccentric thrusts, or complex architectural configurations affecting the structural response.

In conclusion, the investigation highlights the extreme seismic vulnerability of the main facades of the studied churches and underscores the urgent need for targeted retrofit interventions that respect the historical and architectural significance of the structures. Double-sloping façades, accounting for nearly one third of the sample, warrant particular attention as a critical vulnerability pattern within the ecclesiastical heritage. Their geometric configuration, frequently associated with horizontal thrusts generated by vaults and arches and compounded by the lack of effective transverse connections, renders them especially prone to out-of-plane overturning. These observations underscore the importance of prioritizing retrofit interventions for this façade typology, tailored to slenderness, local geometrical characteristics, and the presence of stabilizing structural elements.

Such measures should be calibrated based on slenderness, local geometry, and the presence of counteracting structural elements, aiming to ensure out-of-plane stability and safeguard the cultural heritage of the Sorrentine Peninsula against future seismic events.

CRediT authorship contribution statement

Luigi Amitrano: Writing – original draft, Software, Investigation, Formal analysis, Data curation. **Antonio Formisano:** Writing – review & editing, Visualization, Validation, Supervision, Resources, Project administration, Methodology, Investigation, Funding acquisition, Data curation, Conceptualization. **Giovanna Longobardi:** Writing – original draft, Software, Methodology, Investigation, Formal analysis, Data curation.

Funding

The Authors declare that no funds, grants, or other support were received during the preparation of this manuscript.

Declaration of Competing Interest

The authors declare the following financial interests/personal relationships which may be considered as potential competing interests: Antonio Formisano reports was provided by University of Naples Federico II. If there are other authors, they declare that they have no known competing financial interests or personal relationships that could have appeared to influence the work reported in this paper.

Acknowledgments

The Authors would like to acknowledge the DPC-ReLUIS 2024–2026 research project (WP4 research line) for the financial support to the current research activity.

Data Availability Statement

The data supporting the reported results can be obtained from the authors upon request.

References

[1] Direzione Generale per i Beni Culturali e Paesaggistici, Dipartimento della Protezione Civile, GNDT – Gruppo Nazionale per la Difesa dai Terremoti (2006) Manuale per la compilazione della scheda per il rilievo del danno ai beni culturali – Chiese. Roma: Istituto Poligrafico e Zecca dello Stato..

[2] Colombo P, Santi G. I beni culturali ecclesiastici in Italia. Aggiornamenti Soc 1990: 647–62.

[3] Lo Monaco A, Grillanda N, Onescu I, Fofiu M, Clementi F, D'Amato M, et al. Seismic assessment of Romanian Orthodox masonry churches in the Banat area through a multi-level analysis framework. Eng Fail Anal 2023;146:107111. https://doi.org/10.1016/j.engfailanal.2023.107111.

[4] D'Amato M, Sulla R. Investigations of masonry churches seismic performance with numerical models: application to a case study. Arch Civ Mech Eng 2021;21:161. https://doi.org/10.1007/s43452-021-00312-5.

[5] Amitrano L, Longobardi G, Formisano A. A comprehensive multi-level approach for seismic failure analysis of masonry churches in Sorrento (Naples, Italy). Structures 2025;81:110264.

[6] Lagomarsino S. On the vulnerability assessment of monumental buildings. Bull Earthq Eng 2006;4(4):445–63.

[7] Valente M. Earthquake response and damage patterns assessment of two historical masonry churches with bell tower. Eng Fail Anal 2023;151:107418. https://doi.org/10.1016/j.engfailanal.2023.107418.

[8] Leggieri V, Ruggieri S, Zagari G, Uva G. Appraising seismic vulnerability of masonry aggregates through an automated mechanical-typological approach. Autom Constr 2021;132:103972. https://doi.org/10.1016/j.autcon.2021.103972.

[9] Milani G, Valente M. Failure analysis of seven masonry churches severely damaged during the 2012 Emilia-Romagna (Italy) earthquake: non-linear dynamic analyses vs conventional static approaches. Eng Fail Anal 2015;54:13–56.

[10] Zizi M, Corlito M, Lourenco PB, De Matteis G. Seismic vulnerability of masonry churches in Abruzzi region. Structures 2021;32:662–80.

[11] Todisco P, Ciancio V, Nastri E. Seismic performance assessment of the church of SS. Annunziata in Paestum through finite element analysis. Eng Fail Anal 2024;162: 108388. https://doi.org/10.1016/j.engfailanal.2024.108388.

[12] Okuyucu D, Eslek T, Özdoğan DB, Laçin T, Mercimek Ö, Kocaman İ. Dynamic identification and collapse mechanisms of unreinforced masonry Heritage: a comprehensive study of Erzurum Atatürk House. Eng Fail Anal 2025;180:109850. https://doi.org/10.1016/j.engfailanal.2025.109850.

[13] Vitorino S, Corazzi R, Doz G. Seismic performance assessment of the historical Cathedral of Santa Maria del Fiore Dome by numerical analysis. Eng Fail Anal 2024;165:108734. https://doi.org/10.1016/j.engfailanal.2024.108734.

[14] Moşoarca M, Fofiu M, Onescu I. Failure mechanism of historic churches in Gorj county for shallow seismic action. Eng Fail Anal 2023;152:107502. https://doi.org/10.1016/j.engfailanal.2023.107502.

[15] Doglioni F, Moretti A, Petrini V. Le chiese e il terremoto. Trieste: Edizioni LINT; 1994.

[16] Regione Emilia-Romagna, GNDT-CNR, Istituto di Ricerca sul Rischio Sismico-CNR (1995) Archivio delle chiese danneggiate dal terremoto del 1987 - Province di Modena e Reggio Emilia. CD-ROM..

[17] Lagomarsino S, Brencich A, Bussolino F, Moretti A, Pagnini LC, Podestà S. Una nuova metodologia per il rilievo del danno alle chiese: prime considerazioni sui meccanismi attivati dal sisma. Ing Sismica 1997;3:70–82.

[18] Chiese. Manuale per la compilazione della scheda per il rilievo del danno ai beni culturali. Dipartimento della Protezione Civile; 2006. ⟨https://www.protezionecivile.gov.it/static/aac8c9781e6f66e0414582e52f0545e2/manualechiese.pdf⟩.

[19] Li SQ, Zheng LL. Seismic fragility analysis of building clusters considering the effects of mainshock-aftershock sequences. Struct Saf 2026;118:102647.

[20] Li SQ. Empirical fragility quantification model of regional building portfolios considering optimized seismic intensity measures. Structures 2025;75:108688.

[21] Li SQ, Gardoni P. Optimized seismic hazard and structural vulnerability model considering macroseismic intensity measures. Reliab Eng Syst Saf 2024;252: 110460.

[22] Meglio E, Formisano A. Design and modelling strategy for cold-formed steel exoskeletons for the seismic-energy retrofit of reinforced concrete structures. Structures 2024;69:107502.

[23] Formisano A, Vaiano G, Fabbrocino F, Milani G. Seismic vulnerability of Italian masonry churches: the case of the Nativity of Blessed Virgin Mary in Stellata of Bondeno. J Build Eng 2018;20:179–200.

[24] Ruggieri S, Liguori FS, Leggieri V, Bilotta A, Madeo A, Casolo S, et al. An archetype-based automated procedure to derive global-local seismic fragility of masonry building aggregates: META-FORMA-XL. Int J Disaster Risk Reduct 2023;95: 103903.

[25] Funari MF, Mehrotra A, Lourenço PB. A tool for the rapid seismic assessment of historic masonry structures based on limit analysis optimisation and rocking. Dyn Appl Sci 2021;11:942.

[26] DPCM 09/02/11, Evaluation and reduction of seismic risk of cultural heritage with reference to the Technical Standards for Constructions promulgated by the Ministry of Infrastructure and Transport on 2008 January 14th, 2011..

[27] Betti M, Galano L, Lourenço PB. Territorial seismic risk assessment of a sample of 13 masonry churches in Tuscany (Italy) through simplified indexes. Eng Struct 2021;235:111479.

[28] D'Amato M, Gigliotti R, Laguardia R. Comparative seismic assessment of ancient masonry churches. Front Built Environ 2019;5:56. ⟨https://www.protezionecivile.gov.it/static/178f4bda33a4dc2cc821d71846940079/allegato-schede-plinivs-e-cartis.pdf⟩.

[29] Bartolomei L. Le chiese abbandonate d'Italia: cause, significato, prospettive di gestione. IN_BO. Ricerche e progetti per il territorio. la città e l'architettura 2016;7 (10):6–28.

[30] Dipartimento della Protezione Civile (2023) Classificazione sismica al 31 marzo 2023. ⟨https://rischi.protezionecivile.gov.it/it/sismico/attivita/classificazione-sismica/⟩.

[31] Conferenza Episcopale Italiana (2023) BeWeB - Beni ecclesiastici in web. Chiese in Campania. ⟨https://www.beweb.chiesacattolica.it⟩ (dati aggiornati a luglio 2023).

[32] Regione Campania (2002) Classificazione sismica della regione Campania. Delibera di Giunta Regionale n. 5447 del 07/11/2002.

[33] Dimitri R, De Lorenzis L, Zavarise G. The comparative role of friction in local out-of-plane mechanisms of masonry buildings: pushover analysis and experimental investigation. Eng Struct 2016;126:158–73. https://doi.org/10.1016/j.engstruct.2016.07.024.

[34] Cianchino G, Masciotta MG, De Matteis G, Brando G. Dual approach to large-scale seismic vulnerability assessment of churches through representative archetypes. Heritage 2024;7:6998–7030. https://doi.org/10.3390/heritage7090355.

[35] Szabó S, Funari MF, Casapulla C, Chryssanthopoulos M, Lourenço PB. The role of uncertainties in the seismic assessment of masonry churches affected by compound rocking failure mechanism: macro-block limit analysis investigations. Structures 2024;63:106385.

[36] Casapulla C, Maione A, Argiento LU. Performance-based seismic analysis of rocking masonry façades using non-linear kinematics with frictional resistances: a case study. Int J Archit Herit 2019;15(9):1349–63.

[37] Sorrentino L, Kunnath S, Monti G, Scalora G. Seismically induced one-sided rocking response of unreinforced masonry façades. Eng Struct 2008;30(8): 2140–53.

[38] ⟨https://www.laradice.com/fossa-santa-maria-ad-cryptas/⟩ last access 24/09/2025.

[39] ⟨https://www.foppolimoretta.it/it/gallery/edifici-danneggiati-dal-sisma/chiesa-di-s-biagio-a-s-marino-di-carpi-mo-79/⟩ last access 24/09/2025.

[40] ⟨https://sisma2016.gov.it/2024/09/26/norcia-approvato-lintervento-di-miglioramento-sismico-e-restauro-della-chiesa-di-san-vito-in-agriano/⟩ last access 24/09/2025.

[41] Ministry of Infrastructure and Transport. Technical Standards for Construction; Official Gazette (nr. 42 of 20/02/2018): Rome, Italy, 2018 (In Italian).

[42] Ministerial Circular n.7/2019 (M. C., 02/01/2019). Instructions for the Application of the "Upgrading of Technical Codes for Constructions" (M. D: 17/01/2018). Official Gazette of the Italian Republic published on 2019 January 2nd.

[43] Gelfi P., Arco.exe – Software per la valutazione delle spinte orizzontali. ⟨http://civserv.ing.unibs.it/utenti/gelfi/arco.htm⟩.

[44] Gelfi P. Role of horizontal backfill passive pressure on the stability of masonry vaults. Int J Restor Build 2002;8(6):573–89.

[45] Giuffrè A. (2003) La meccanica nell'architettura. La statica. Roma: Gangemi Editore.